Preprints of the 21st IFAC World Congress (Virtual)
Berlin, Germany, July 12-17, 2020

Uniform global asymptotic synchronization of Kuramoto oscillators via hybrid coupling

R. Bertollo [*] **E. Panteley** [**] **R. Postoyan** [***] **L. Zaccarian** [*,****]

[*] *Dipartimento di Ingegneria Industriale, University of Trento, Italy (e-mail: riccardo.bertollo@unitn.it)*
[**] *CNRS, L2S, Gif-sur-Yvette, France (e-mail: panteley@centralesupelec.fr)*
[***] *Université de Lorraine, CNRS, CRAN, Nancy, France (e-mail: romain.postoyan@univ-lorraine.fr)*
[****] *CNRS, LAAS, Université de Toulouse, 31400 Toulouse, France (e-mail: zaccarian@laas.fr).*

Abstract: Using a hybrid framework, we propose a generalized version of the well-known Kuramoto model for interconnected oscillators. The proposed model does not modify the classical model close to the synchronization set, but avoids the typical non-uniform convergence phenomenon. For the two-oscillators case, we prove the uniform global asymptotic stability of the consensus set by using a hybrid Lyapunov function whose generality promises possible extension of the result to higher order dynamics. We comparatively illustrate the achieved uniform convergence properties by simulating both the case with two and multiple oscillators, thus confirming the effectiveness of our approach.

Keywords: Kuramoto model, hybrid systems, nonlinear control, networked oscillators, synchronization

1. INTRODUCTION

Complex systems with oscillatory behavior are omnipresent in nature and appear in various engineering applications. Among various models proposed to describe dynamics of such systems, perhaps the most popular one is due to Kuramoto (1975) who suggested a simple model of globally "all-to-all" coupled phase oscillators

$$\dot{\theta}_i = \omega_i + \frac{K}{n}\sum_j \sin(\theta_j - \theta_i), \qquad i \in \{1, \dots, n\}, \qquad (1)$$

where θ_i and ω_i are respectively the phase and the natural frequency of the i-th oscillator and K is the coupling strength.

Model (1) is now widely known as "Kuramoto model" and has been used in numerous applications in biology, chemistry, physics and medicine. As examples we cite here deep brain stimulation in Tass (2003) and synchronization of coupled Josephson junctions in Wiesenfeld et al. (1998), for more examples see e.g. Acebron et al. (2005) and Strogatz (2000). More recently, it has also attracted the attention from the automatic control community, see e.g. Aeyels and Rogge (2004), Sepulchre et al. (2007), Chopra and Spong (2009), Jadbabaie et al. (2004). The popularity of this model probably stems from the fact that it offers a benchmark description of oscillatory systems.

Stability properties of the Kuramoto model have been explored extensively during the last 40 years, including bounds on the interconnections terms, explicit expressions for the asymptotic phase offset and stability issues, see Strogatz (2000) and Dörfler and Bullo (2011) for detailed overviews. Generalizations of the Kuramoto model to the networks where nodes have more complex dynamics was proposed e.g. in Dörfler and Bullo (2010) for the stability analysis of power networks, and the case of more complex coupling gains was considered e.g. in Leonard et al. (2012) for the analysis of collective decisions about the movement direction in groups of animals as well as in Aoki (2015) to describe neuronal networks with synaptic plasticity.

Since the coupling sine function in (1) vanishes when the phase differences approach π, in the case of equal natural frequencies ω_i (i.e. $\omega_i = \omega$ for any $i \in \{1, \dots, n\}$) the system possesses multiple synchronization sets, see e.g. Sepulchre et al. (2007). As a result, slow convergence is observed when simulating solutions starting close to the unstable synchronization sets (e.g., two oscillators with phase opposition). This is due to the uniqueness of solutions of dynamics (1) combined with continuity properties of solutions with respect to initial conditions on compact time intervals. Roughly speaking, the closer solutions start to the unstable synchronization set, the longer it will take them to get move away from that set and finally converge to the synchronized motion. As a result, the convergence properties of solutions is not uniform over all initial conditions. A similar non-uniform convergence behavior can be observed in the example of synchronizing metronomes Oud (2006) where the dynamics is of higher order but similar phenomena occur. Even though such a behaviour can be acceptable to describe certain natural phenomena, it is less suitable for many engineering applications. For example such a stickiness effect is well known in certain engineering areas (e.g., control of unstable aircraft dynamics) wherein solutions are kept at a safe distance from the boundaries of the null controllability region Miller and Pachter (1997).

With this motivation in mind, we propose here a generalization of the Kuramoto model using a hybrid framework similarly to what has been done for spiking interconnected neurons in Phillips and Sanfelice (2014). Our model does not modify dynamics (1) close to the stable synchronization set and it guarantees uniform convergence even when

[1] This work is supported by HANDY project ANR-18-CE40-0010.

the initial synchronization errors are large. In particular, by introducing some discrete jumps that exploit the periodicity of the oscillators phases, we force variables θ_i to evolve in a bounded region of the state space. Because of this periodicity, we need to keep track of the unwinding between the states, therefore we introduce a number of discrete states k_{ij} whose role is to preserve continuity of the argument of the (continuous-time) coupling functions across jumps of the state variables θ_i.

We also formulate basic properties that our hybrid coupling should satisfy to ensure uniform global asymptotic stability (UGAS) of the synchronization set for our hybrid Kuramoto model. In particular, UGAS comprises uniform global attractivity, which is exactly the property that the original Kuramoto model in (1) fails to satisfy.

The paper is organized as follows. In Section 2 we focus on a simple network composed of two oscillators and carry out detailed stability analysis for this model based on a suitable hybrid Lyapnuov function. We generalize our approach to the case of n oscillators in Section 3, where we do not provide a parallel stability analysis, whose technical details are left as future work. Numerical simulations are then presented in Section 3.3 to illustrate the advantages of the proposed hybrid model. Due to space reasons all the proofs are omitted, but can be found in the extended version of this paper, available at Bertollo et al. (2020).

Notation: $\mathbb{R}^n$ denotes the n-dimensional Euclidean space. $\mathbb{R}_{\geq 0}$ denotes the set of nonnegative real numbers. $\mathbb{Z}$ denotes the set of all integers, while $\mathbb{Z}_{\geq 0}$ denotes the set of nonnegative integers. Given two vectors x_1 and x_2, we denote $(x_1, x_2) = [x_1^T \ x_2^T]^T$.

2. THE CASE OF TWO OSCILLATORS

2.1 Flow dynamics

Consider two coupled oscillators whose continuous (flowing) evolution is ruled by the following generalization of (1) (in this preliminary work we consider oscillators with homogeneous natural frequencies, namely $\omega_i = \omega$, $i \in \{1, 2\}$):

$$\begin{bmatrix} \dot{\theta}_1 \\ \dot{\theta}_2 \end{bmatrix} = \begin{bmatrix} \omega + \gamma\sigma(\theta_2 - \theta_1 + 2k_{12}\pi) \\ \omega - \gamma\sigma(\theta_2 - \theta_1 + 2k_{12}\pi) \end{bmatrix}, \quad (\theta_1, \theta_2, k_{12}) \in C, \tag{2}$$

where γ is a positive gain, associated to the intensity of the coupling action.

In (2), the state of the overall coupled system corresponds to $x := (\theta_1, \theta_2, k_{12})$, where θ_i, $i \in \{1, 2\}$ are the two phases and $k_{12} \in \{-2, -1, 0, 1, 2\}$, satisfying $\dot{k}_{12} = 0$, is a logical state whose jumps unwind the phase difference between the two oscillators (dynamics (1) is recovered when $k_{12} = 0$). The reason for inserting k_{12} in the dynamics is that it can constrain flowing to only happen when $(\theta_1, \theta_2, k_{12}) \in C$, with C (to be precisely characterized later) satisfying the next property.

$$C \subset \big\{x : |\theta_2 - \theta_1 + 2k_{12}\pi| \leq \pi + \delta\big\}. \tag{3}$$

The scalar $\delta \in (0, 2\pi/3]$ in (3) is an arbitrary positive angle ensuring space regularization to prevent Zeno solutions. The value of δ has some marginal impact on the transient responses from large initial conditions, but has no impact on local solutions around the attractor. For example, in our simulations we select $\delta = \frac{\pi}{4}$.

The advantage of (2) versus (1) is that property (3) ensures that during the continuous evolution (flow) of the solutions, function σ is only evaluated in the compact set $[-\pi - \delta, \pi + \delta]$ and therefore we may replace the sine function of (1) by more advantageous functions not suffering from the issue of vanishing at π. In particular, the uniform synchronization results of this paper hold as long as σ satisfies the following property.

Property 1. Function σ is continuous on $\operatorname{dom}\sigma := [-\pi - \delta, \pi + \delta]$ and satisfies

(i) $\sigma(s) = -\sigma(-s)$, for any $s \in \operatorname{dom}\sigma$
(ii) $\sigma(s)s > 0$, for any $s \in \operatorname{dom}\sigma \setminus \{0\}$

Remark 1. Item (i) of Property 1 can be removed, at the cost of making our proofs more convoluted in terms of notation. Item (ii) with continuity implies $\sigma(0) = 0$ for any σ satisfying Property 1. ⌟

An example of function σ that satisfies Property 1 and that perfectly matches the one in classical Kuramoto oscillators like (1) near the synchronization set, corresponds to

$$\sigma : \theta \mapsto \begin{cases} \sin(\theta), & \text{if } |\theta| \leq \dfrac{\pi}{2} \\ \operatorname{sgn}(\theta) & \text{if } |\theta| \in [\pi/2, \pi + \delta], \end{cases} \tag{4}$$

Once again, under condition (3), the argument of σ never has norm larger than $\pi + \delta$ in places where solutions are allowed to evolve continuously (flow), so there is no need to define function σ outside $\operatorname{dom}\sigma := [-\pi - \delta, \pi + \delta]$.

We now precisely introduce the proposed flow dynamics. The overall state evolves (continuously or discretely) in the (bounded) state space defined as

$$X := [-\pi, \pi]^2 \times \{-2, -1, 0, 1, 2\}. \tag{5}$$

Based on (2), the continuous motion of x is ruled by

$$\dot{x} = \begin{bmatrix} \dot{\theta}_1 \\ \dot{\theta}_2 \\ \dot{k}_{12} \end{bmatrix} = f(x) := \begin{bmatrix} \omega + \gamma\sigma(\theta_2 - \theta_1 + 2k_{12}\pi) \\ \omega - \gamma\sigma(\theta_2 - \theta_1 + 2k_{12}\pi) \\ 0 \end{bmatrix}. \tag{6}$$

2.2 Jump dynamics

A few jump rules are now introduced to ensure that solutions are well defined, i.e. that maximal solutions are complete, while ensuring (3). A graphical representation of these sets is shown in Figure 1. First, we consider the next jump dynamics

$$\begin{bmatrix} \theta_1^+ \\ \theta_2^+ \\ k_{12}^+ \end{bmatrix} = g_1(x) := \begin{bmatrix} g_\theta(\theta_1) \\ \theta_2 \\ k_{12} - \operatorname{sgn}(\theta_1) \end{bmatrix}, \quad x \in D_1 \tag{7a}$$

$$\begin{bmatrix} \theta_1^+ \\ \theta_2^+ \\ k_{12}^+ \end{bmatrix} = g_2(x) := \begin{bmatrix} \theta_1 \\ g_\theta(\theta_2) \\ k_{12} + \operatorname{sgn}(\theta_2) \end{bmatrix}, \quad x \in D_2, \tag{7b}$$

where the jump sets D_1 and D_2 and function g_θ are defined as follows, for $i \in \{1, 2\}$,

$$D_i := \big\{x \in X : |\theta_i| \in [\pi + \delta, 2\pi]\big\}, \tag{7c}$$

$$g_\theta(\theta_i) := \theta_i - \operatorname{sgn}(\theta_i)2\pi, \tag{7d}$$

where X is defined in (5). Note that g_θ, g_1 and g_2 are continuous on their (not connected) domain, because D_i does not contain any point $x = (\theta_1, \theta_2, k_{12})$ with $\theta_i = 0$.

The rationale behind the jump laws in (7) is that the oscillators coordinates θ_i are forced to jump whenever they point outside the set $[-\pi - \delta, \pi + \delta]$, see the definition of D_i in (7c). Moreover, these jumps are multiples of 2π in view of the definition of g_θ in (7d), so that they do not correspond to any angular jump. Finally, the jumps of k_{12} are enforced according to g_1 and g_2 in (7a) and (7b), in such a way that the argument of σ in (6) remains constant

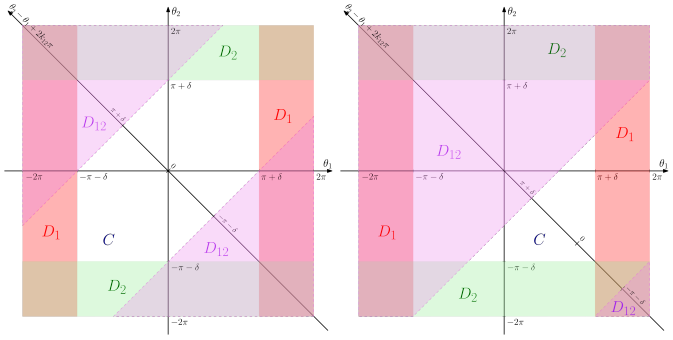

(a) Case with $k_{12} = 0$. (b) Case with $k_{12} = 1$.

Fig. 1. A visual example of the flow and jump sets, for different values of k_{12}.

across such jumps. In other words, the right hand side in (6) remains continuous across jumps.

State k_{12} is also subject to jumps ensuring that the argument of function σ in (6) has norm no larger than $\pi + \delta$. These jumps are triggered on the set

$$D_{12} := \{x \in X : \min_{h\in\mathbb{Z}} |\theta_2 - \theta_1 + 2h\pi| \leq |\theta_2 - \theta_1 + 2k_{12}\pi| - 2\delta\}, \quad (8)$$

and correspond to the following jump map, essentially induced by the above selection of D_{12}, which does not affect θ_1 and θ_2 but only k_{12}

$$\begin{bmatrix}\theta_1^+\\ \theta_2^+\\ k_{12}^+\end{bmatrix} \in G_{12}(x) := \begin{bmatrix}\theta_1\\ \theta_2\\ \operatorname*{argmin}_{h\in\mathbb{Z}} |\theta_2 - \theta_1 + 2h\pi|\end{bmatrix}. \quad (9)$$

Note that G_{12} in the above selection is a set-valued map because there may be more than one minimizer of the function $|\theta_2 - \theta_1 + 2h\pi|$.

2.3 Overall model and its structural properties

The hybrid formulation of the two coupled oscillators is completed by writing the data of the following general form

$$\begin{cases}\dot{x} = f(x), & x \in C,\\ x^+ \in G(x), & x \in D,\end{cases} \quad (10a)$$

where f is defined in (6), the flow and jump sets are defined to prioritize jumps

$$D := D_1 \cup D_2 \cup D_{12}, \quad (10b)$$

$$C := \overline{X \setminus D}, \quad (10c)$$

where X is defined in (5). Finally, the jump map G is a set-valued map defined in terms of its graph, which is selected as the union of the graphs of g_1, g_2, and G_{12}

$$\operatorname{gph} G = \operatorname{gph} g_1 \cup \operatorname{gph} g_2 \cup \operatorname{gph} G_{12}. \quad (10d)$$

Figure 1 shows the state space X projected on the (θ_1, θ_2) plane for two values of k_{12}, highlighting the flow set and the different jump sets.

Dynamics (10a) enjoys a few useful properties. First, the set C in (10c) satisfies (3) (as proven in (Bertollo et al., 2020, Lemma 1)) so that it is not necessary to define σ outside $\operatorname{dom}\sigma := [-\pi - \delta, \pi + \delta]$. Moreover, it enjoys the hybrid basic conditions of (Goebel et al., 2012, Chapter 6), as proved in (Bertollo et al., 2020, Lemma 2), ensuring sequential compactness of solutions, and intrinsic robustness of asymptotic stability. Finally, the following lemma is a key step to be able to prove Theorem 1 below. We number it consistently with the same result in (Bertollo et al., 2020, Lemma 3), where its proof is reported.

Lemma 3. For each initial condition, there exists at least one complete solution to hybrid system (10). Moreover, no complete solution ϕ exists that never flows (it is discrete) and only jumps according to (7a) or (7b).

Remark 2. Since some maximal solutions to hybrid system (10) are not complete, from now on we add the prefix "pre" when referring to the stability properties, i.e. *uniform global pre-asymptotic stability (UGpAS)*. Based on its use in Goebel et al. (2012), the prefix "pre" highlights that complete solutions asymptotically converge to the attractor, but it is possible that some maximal solutions are not complete. ⌟

2.4 Uniform stability guarantees

We can now state the main uniform stability theorem for dynamics (10).

Theorem 1. The following synchronization set

$$\mathcal{A} := \{x \in X : \theta_1 = \theta_2 + 2k_{12}\pi, k_{12} \in \{-1, 0, 1\}\} \quad (11)$$

is uniformly globally pre-asymptotically stable (UGpAS) for dynamics (10).

Recall from (Goebel et al., 2012, Definition 3.6) that UGpAS of a closed set is given by the combination of uniform global stability (UGS) and uniform global pre-attractivity (UGpA). While UGS ensures stability, or boundedness, of the solutions starting from any initial condition, UGpA guarantees uniform convergence to the attractor for any complete solution. UGpA cannot be ensured with the classical continuous description, and represents the main advantage of the proposed hybrid approach. In addition, in view of (Goebel et al., 2012, Theorem 7.21), the attractor $\mathcal{A}$ is robustly pre-asymptotically stable, see (Goebel et al., 2012, Definition 7.15), since it is UGpAS and compact, and system (10) is well-posed, as emphasized above.

Theorem 1 does not impose any constraint on the coupling gain $\gamma > 0$; this is because of the uniform ω for the two oscillators, and the result is in line with the one obtained with the classical approach in works like e.g. Dörfler and Bullo (2011). Based on this work, we expect the value of γ to be related to the convergence rate, and in a possible extension with non-uniform values of ω we expect the results to hold for a sufficiently large value of γ.

Sketch of the proof of Theorem 1 (a complete proof is reported in (Bertollo et al., 2020, §2.5)). Consider the set

$$\mathcal{A}' := \{x \in X : \theta_1 = \theta_2 + 2k_{12}\pi\} \supset \mathcal{A} \quad (12)$$

and the Lyapunov function candidate

$$V(x) := \int_0^{\operatorname{sat}_{\pi+\delta}(\theta_2 - \theta_1 + 2k_{12}\pi)} \sigma(s)ds, \quad \forall x \in X, \quad (13)$$

where X is given in (5). From Property 1, function V is well defined on X and zero in $\mathcal{A}'$ and positive elsewhere. Additionally, V is vacuously radially unbounded, because its domain is a compact set.

Along flowing solutions, due to (3), in view of (6) and (13), we have, for all $x \in C \setminus \mathcal{A}'$,

$$\langle \nabla V(x), f(x)\rangle = -2\gamma\sigma(\theta_2 - \theta_1 + 2k_{12}\pi)^2 < 0, \quad (14)$$

see (Bertollo et al., 2020, §2.5) for the details. On the other hand, carefully considering each jump map and jump set, it is proven in (Bertollo et al., 2020, §2.5) that

$$V(g) \leq V(x), \quad \forall x \in D, \forall g \in G(x), \quad (15)$$

and that no complete solution ξ exists satisfying $V(\xi(t, j)) = V(\xi(0, 0)) \neq 0$, for all $(t, j) \in \operatorname{dom}\xi$. Thus, set $\mathcal{A}'$ is

UGpAS using the hybrid invariance principle in (Seuret et al., 2019, Thm 1).

As a last step, it is proven in (Bertollo et al., 2020, §2.5) that $\mathcal{A}$ is strongly forward invariant and uniformly attractive from $\mathcal{A}'$. Therefore, using a global version of (Goebel et al., 2012, Prop. 7.5), we conclude UGpAS of $\mathcal{A}$ from $\mathcal{A}'$.

Finally, UGpAS of $\mathcal{A}'$ combined with UGpAS of $\mathcal{A}$ from $\mathcal{A}'$, together with boundedness of solutions from boundedness of X, implies UGpAS of $\mathcal{A}$ due to (Maggiore et al., 2019, Corollary 4.8). ■

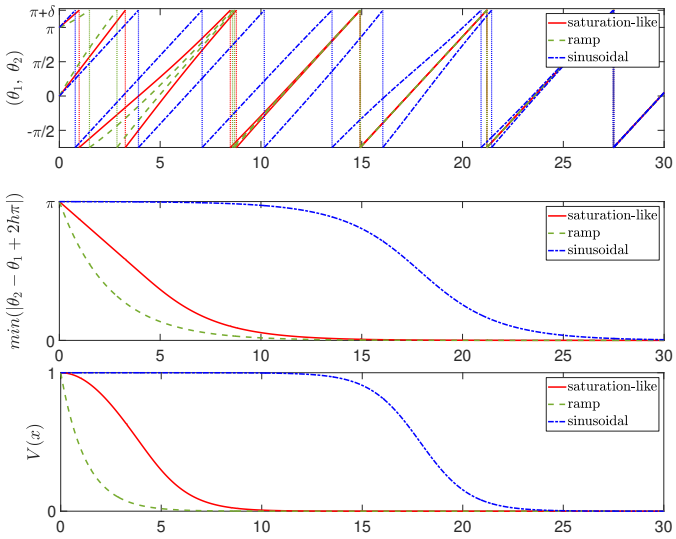

Fig. 2. Results of simulations: two oscillators, $\omega = 1$, $\gamma = 0.2$, initial phase difference of about π.

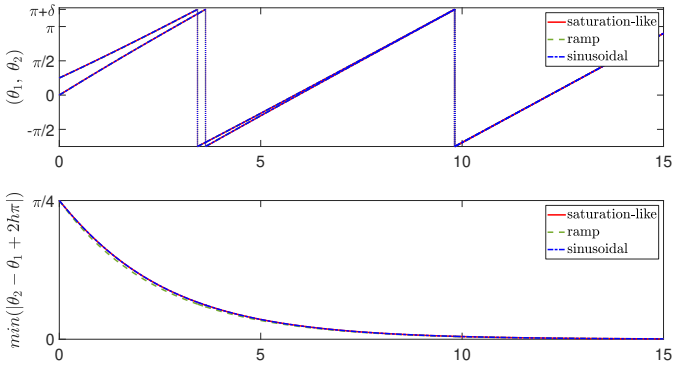

Fig. 3. Results of simulations: two oscillators, $\omega = 1$, $\gamma = 0.2$, initial phase difference of $\pi/4$.

2.5 Simulation results

We provide results of simulations carried out with the Matlab add-on Hybrid Equations Toolbox, Sanfelice et al. (2013). We first show in Figure 2, the evolution of θ_1 and θ_2, using different coupling functions corresponding to sinusoidal coupling (blue dash-dotted), a linear ramp coupling (green dashed) and the coupling function in (4) (red solid). See also (Bertollo et al., 2020, Fig. 1).

The three graphs show the evolution of the oscillators phases (top), the value of the angular error (middle) and the value of the Lyapunov function defined in (13) (bottom), normalized with the initial value so that the numerical values are comparable for different functions σ. We can see the slow initial error transient with sinusoidal coupling: a visual evidence of the non-uniform attractivity of the synchronization set when σ does not satisfy Property 1 and trajectories start close to the unstable desynchronized evolution.

We now select the initial condition of these simulations closer to the equilibrium, in particular the initial phase difference is $\pi/4$. The results are shown in Figure 3. Since the evolution of the Lyapunov function along the solution is qualitatively similar to the evolution of the angular error, we only show the angular error. In this case the solutions behave very similarly for the three coupling functions, which is in line with our idea of not modifying the dynamics near the equilibrium.

3. GENERALIZATION TO n OSCILLATORS

In this section, we consider the general case where $n \in \mathbb{Z}, n \geq 2$ oscillators are interconnected via hybrid coupling over a directed graph. We first need to recall some background on graph theory for this purpose.

3.1 Background on graph theory

We denote an unweighted undirected graph $\mathcal{G} = (\mathcal{V}, \mathcal{E})$, where $\mathcal{V}$ is the set of vertices, or nodes, and $\mathcal{E}$ is the set of edges, or arcs, composed by unordered couples of nodes. If a couple of nodes belongs to $\mathcal{E}$, those nodes are adjacent.

Moreover, we denote (unweighted) directed graphs $\mathcal{G}_o = (\mathcal{V}, \mathcal{E})$, where $\mathcal{E} \subseteq \mathcal{V} \times \mathcal{V}$ is composed of ordered couples, so arcs have a specific direction. An arc going from node i to node j is denoted by $(i, j) \in \mathcal{E}$. If a directed graph $\mathcal{G}_o$ is obtained choosing an arbitrary direction for the edges of an undirected graph $\mathcal{G}$, we call it an oriented graph, and we say that $\mathcal{G}_o$ is obtained from an orientation of $\mathcal{G}$.

Given a directed graph, if $(i, j) \in \mathcal{E}$ we say that i belongs to the set of in-neighbors $\mathcal{I}_j$ of j, while j belongs to the set of out-neighbors $\mathcal{O}_i$ of i. The union of $\mathcal{I}_i$ and $\mathcal{O}_i$ gives the more generic set of neighbors $\mathcal{N}_i := \mathcal{I}_i \cup \mathcal{O}_i$ of node i, containing all the nodes connected to it, in any direction. Given two nodes x and y of an undirected graph $\mathcal{G}$, we define as path from x to y a set of vertices starting with x and ending with y, such that consecutive vertices are adjacent. If there is a path between any couple of nodes, $\mathcal{G}$ is called connected, otherwise it is called disconnected. Given an unweighted directed graph G with $n = |\mathcal{V}|$ vertices and $m = |\mathcal{E}|$ edges, $B \in \mathbb{R}^{n \times m}$ is its incidence matrix, where each column $[B]_\ell, \ell \in \{1, \dots, m\}$ is associated to an edge $(i, j) \in \mathcal{E}$, and all entries of $[B]_\ell$ are zero except for $b_{i\ell} = -1$ (the tail of edge ℓ) and $b_{j\ell} = 1$ (the head of edge ℓ), namely

$$[B]_\ell = e_j - e_i, \tag{16}$$

where e_i is the i-th natural base of $\mathbb{R}^n$.

3.2 Hybrid model

To generalize the two agents dynamics described in Section 2 we use an undirected graph $\mathcal{G} = (\mathcal{V}, \mathcal{E}_u)$ and arbitrarily choose an orientation for its edges, obtaining the oriented graph $\mathcal{G}_o = (\mathcal{V}, \mathcal{E})$. We consider n oscillators, each one associated to a state $\theta_i, i \in \mathcal{V} = \{1, \dots, n\}$, and m discrete states k_{ij}, $(i, j) \in \mathcal{E}$, associated to each one of the m connections among the oscillators, representing the unwinding between θ_i and θ_j. The state of this system can be therefore represented as

$$x := (\theta, k) \in X := [-2\pi, 2\pi]^n \times \{-2, -1, 0, 1, 2\}^m, \tag{17}$$

where $\theta := (\theta_1, \dots, \theta_n) \in \mathbb{R}^n$, and $k \in \{-2,-1,0,1,2\}^m$ contains an ordered list of all the k_{ij}s, $(i,j) \in \mathcal{E}$, with an ordering that coincides with the ordering of the columns of B in (16).

To simplify the notation, inspired by (6), given a function σ satisfying Assumption 1, we introduce for any $\theta \in \mathbb{R}^n$ and $k \in \mathbb{R}^m$

$$\sigma_{ij} := \sigma(\theta_j - \theta_i + 2k_{ij}\pi) \tag{18}$$

and we arrange these functions in a vector $\boldsymbol{\sigma} \in \mathbb{R}^m$, with an ordering that coincides with the ordering of the columns of B in (16). From the definitions above, we can write the following generalization of (6), which covers as a special case the model treated in Section 2 with $\mathcal{V} = \{1,2\}$ and one edge $\mathcal{E} = \{(1,2)\}$

$$\begin{aligned} \dot\theta_i = f_i(x) :=\ & \omega + \gamma \sum_{h\in\mathcal{O}_i} \sigma_{ih} - \gamma \sum_{h\in\mathcal{I}_i} \sigma_{hi} && (19)\\ =\ & \omega - \gamma (B)_i \boldsymbol{\sigma}, && \forall i \in \mathcal{V},\\ \dot k_{ij} =\ & 0, && \forall (i,j) \in \mathcal{E}, \quad (20) \end{aligned}$$

where $(B)_i$ denotes the i-th row of matrix B and the second line of (19) comes from (16) and the ordering of $\boldsymbol{\sigma}$. Equations (19) and (20) can be written compactly as

$$\begin{cases} \dot\theta = \omega \mathbf{1}_n - \gamma B \boldsymbol{\sigma}, \\ \dot k = 0, \end{cases} \tag{21}$$

where $\mathbf{1}_n \in \mathbb{R}^n$ represents the column vector of ones.

The jump rules follow the same logic as the ones defined in (7) and (8), which is generalized as

$$x^+ = g_i(x) := \begin{bmatrix} g_{i,\theta}(x) \\ g_{i,k}(x) \end{bmatrix}, \qquad x \in D_i \tag{22a}$$

$$x^+ \in G_{ij}(x) := \begin{bmatrix} \theta \\ G_{ij,k}(x) \end{bmatrix}, \qquad x \in D_{ij} \tag{22b}$$

where the entries of $g_{i,\theta} : X \to [-2\pi, 2\pi]^n$ and $g_{i,k} : X \to \{-2,-1,0,1,2\}^m$ are defined as

$$(g_{i,\theta})_j = \begin{cases} g_\theta(\theta_i), & \text{if } j = i, \\ \theta_j, & \text{otherwise.} \end{cases} \tag{22c}$$

$$(g_{i,k})_{(u,v)} = \begin{cases} k_{uv} + \operatorname{sgn}(\theta_i), & \text{if } v = i, \\ k_{uv} - \operatorname{sgn}(\theta_i), & \text{if } u = i, \\ k_{uv}, & \text{otherwise,} \end{cases} \tag{22d}$$

where g_θ is defined in (7d). On the other hand, the entries of $G_{ij,k} : X \rightrightarrows \{-2,-1,0,1,2\}^m$ are given by

$$(G_{ij,k})_{(u,v)} = \begin{cases} \operatorname*{argmin}_{h\in\mathbb{Z}} |\theta_j - \theta_i + 2h\pi|, & \\ & \text{if } (u,v) = (i,j), \\ k_{uv}, & \text{otherwise.} \end{cases} \tag{22e}$$

Finally sets D_i, $i \in \{1,\dots,n\}$ and D_{ij}, $(i,j) \in \mathcal{E}$ generalize (7c) and (8) as

$$D_i := \{x \in X : |\theta_i| \in [\pi + \delta, 2\pi]\} \tag{22f}$$

$$\begin{aligned} D_{ij} := \{x \in X :\ & \min_{h\in\mathbb{Z}} |\theta_j - \theta_i + 2h\pi| \\ & \le |\theta_j - \theta_i + 2k_{ij}\pi| - 2\delta\}. \end{aligned} \tag{22g}$$

To complete the hybrid formulation, we may write the equations in the general form (10a), with

$$f(x) = (f_1(x), \dots, f_n(x), 0, \dots, 0), \tag{23a}$$

G is defined in terms of its graph as in (10d), namely

$$\operatorname{gph} G := \left(\bigcup_{i=1}^n \operatorname{gph} g_i \right) \cup \left(\bigcup_{(i,j)\in\mathcal{E}} \operatorname{gph} G_{ij} \right), \tag{23b}$$

and the jump/flow sets, generalizing (10b) and (10c),

$$D := \left(\bigcup_{i=1}^n D_i \right) \cup \left(\bigcup_{(i,j)\in\mathcal{E}} D_{ij} \right), \tag{23c}$$

$$C := \overline{X \setminus D}. \tag{23d}$$

Remark 3. Similar to the two oscillators case, for the generalized flow set in (23d), it holds that

$$C \subset \{x : |\theta_j - \theta_i + 2k_{ij}\pi| \le \pi + \delta\} \tag{24}$$

so that the flow map is only evaluated with the argument of σ within $\operatorname{dom}\sigma$. ⌟

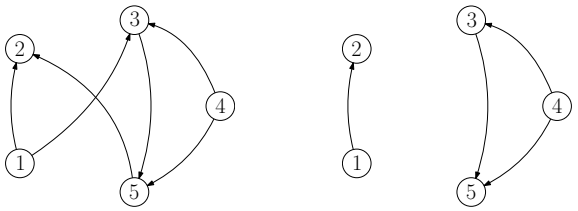

(a) Connected graph. (b) Disconnected graph.

Fig. 4. The oriented graphs in the simulations with $n = 5$.

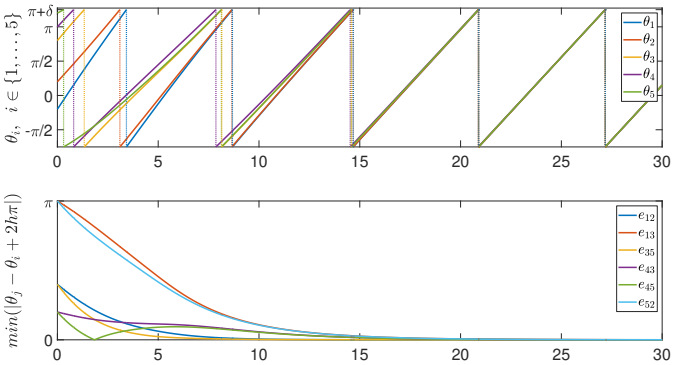

Fig. 5. Simulation with five oscillators, $\omega = 1$ and $\gamma = 0.2$, connected graph, coupling function described in (4).

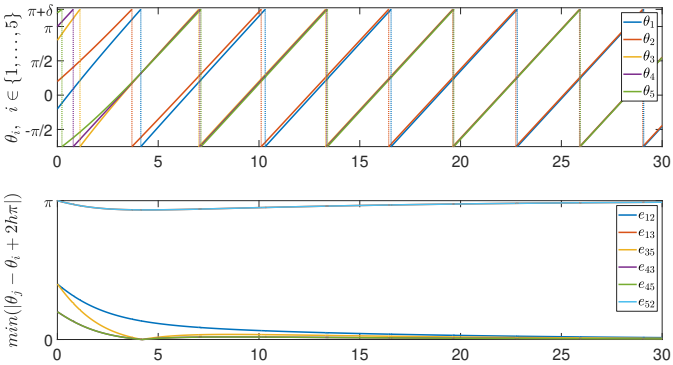

Fig. 6. Simulation with five oscillators, $\omega = 1$ and $\gamma = 0.2$, connected graph, sinusoidal coupling function.

3.3 Simulation results

We consider five coupled oscillators, as an example of the generalized system described above.

We first study the evolution of a system described by the graph in Figure 4a, which is obtained as an orientation of a connected undirected graph. Simulations have been performed both for the coupling function in (4) and for

the typical sinusoidal coupling function. The results are depicted in Figures 5-6, respectively. Comparing the two figures, it is apparent that for this particular graph structure and initial conditions, the sinusoidal coupling results in extremely slow convergence (due to the non-uniform convergence properties emphasized in our introduction). Instead, the proposed hybrid model appears to maintain uniform convergence properties. It is emphasized that for alternative initial conditions, also the sinusoidal couplings provide comparable synchronization transients to the ones of Figure 5. As a matter of fact, for not-so-large initial conditions we find similar results to those of Figure 3 wherein the two systems provide the same evolution.

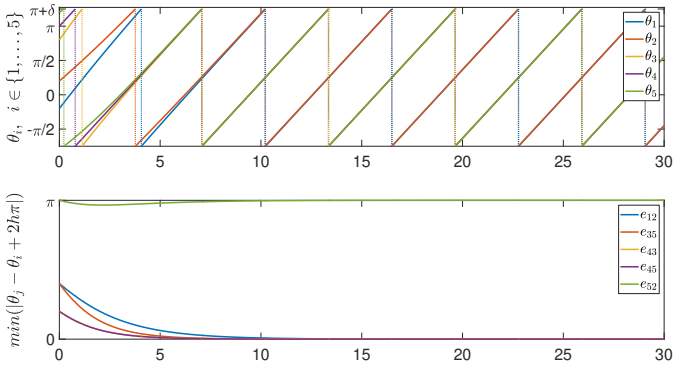

Fig. 7. Simulation with five oscillators, $\omega = 1$ and $\gamma = 0.2$, disconnected graph.

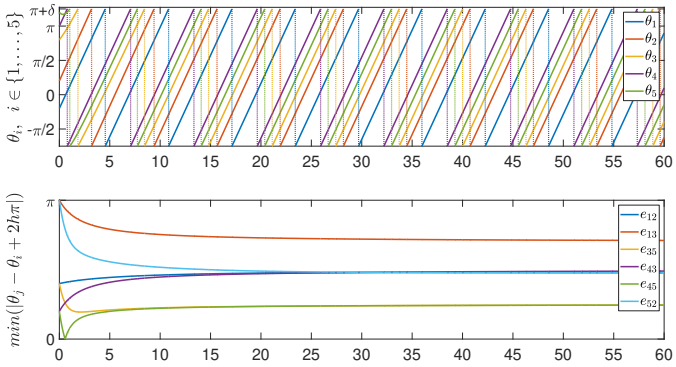

Fig. 8. Simulation with five oscillators, $\omega = 1$ and $\gamma = 1$, directed graph.

We also study some examples associated to natural extensions of this work: the first one is a system described by the graph in Figure 4b, obtained by orienting a disconnected undirected graph. The corresponding results are shown in Figure 7: the phase errors converge to zero for the connected elements, but if we consider the difference between states belonging to different connected components of the graph (phases θ_2 and θ_5 in our case) the error does not converge. A second extension concerns the case of a system with directed connections: the graph structure is again the one in Figure 4a, but the coupling function is applied only to the head of each edge. We can see from the results in Figure 8 that synchronization is not achieved in this case.

Acknowledgment: The authors thank Simone Mariano for the useful discussions about the final manuscript.

REFERENCES

Acebron, J.A., Bonilla, L.L., Vicente, C.J.P., Ritort, F., and Spigler, R. (2005). The Kuramoto model: A simple paradigm for synchronization phenomena. *Reviews of Modern Physics*, 77(1), 137–185.

Aeyels, D. and Rogge, J.A. (2004). Existence of partial entrainment and stability of phase locking behavior of coupled oscillators. *Pr. of Theor. Phys.*, 112, 921–942.

Aoki, T. (2015). Self-organization of a recurrent network under ongoing synaptic plasticity. *Neural Networks*, 62, 11–19.

Bertollo, R., Panteley, E., Postoyan, R., and Zaccarian, L. (2020). Uniform global asymptotic synchronization of kuramoto oscillators via hybrid coupling. *HAL Technical Report*, HAL-02562689.

Chopra, N. and Spong, M.W. (2009). On exponential synchronization of Kuramoto oscillators. *IEEE transactions on Automatic Control*, 54(2), 353–357.

Dörfler, F. and Bullo, F. (2010). Synchronization and transient stability in power networks and non-uniform Kuramoto oscillators. *SIAM Journal on Control and Optimization*, 50(3), 1616–1642.

Dörfler, F. and Bullo, F. (2011). On the critical coupling for Kuramoto oscillators. *SIAM Journal on Control and Optimization*, 10(3), 1070–1099.

Goebel, R., Sanfelice, R., and Teel, A. (2012). *Hybrid Dynamical Systems: modeling, stability, and robustness*. Princeton University Press.

Jadbabaie, A., Motee, N., and Barahona, M. (2004). On the stability of the Kuramoto model of coupled nonlinear oscillators. In *Proceedings of the 2004 American Control Conference*, volume 5, 4296–4301. IEEE.

Kuramoto, Y. (1975). Self-entrainment of a population of coupled non-linear oscillators. In *International symposium on mathematical problems in theoretical physics*, 420–422. Springer.

Leonard, N.E., Shen, T., Nabet, B., Scardovi, L., Couzin, I.D., and Levin, S.A. (2012). Decision versus compromise for animal groups in motion. *Proceedings of the National Academy of Sciences*, 109(1), 227–232.

Maggiore, M., Sassano, M., and Zaccarian, L. (2019). Reduction theorems for hybrid dynamical systems. *IEEE Transactions on Automatic Control*, 64(6), 2254–2265.

Miller, R. and Pachter, M. (1997). Maneuvering flight control with actuator constraints. *Journal of guidance, control, and dynamics*, 20(4), 729–734.

Oud, W.T. (2006). *Design and experimental results of synchronizing metronomes, inspired by Christiaan Huygens*. Master's Thesis, Eindhoven University of Technology.

Phillips, S. and Sanfelice, R.G. (2014). A framework for modeling and analysis of dynamical properties of spiking neurons. In *American Control Conference*.

Sanfelice, R., Copp, D., and Nanez, P. (2013). A toolbox for simulation of hybrid systems in Matlab/Simulink: Hybrid Equations (HyEQ) Toolbox. In *Proceedings of the 16th international conference on Hybrid systems: computation and control*, 101–106. ACM.

Sepulchre, R., Paley, D.A., and Leonard, N.E. (2007). Stabilization of planar collective motion: All-to-all communication. *IEEE Transactions on Automatic Control*, 52(5), 811–824.

Seuret, A., Prieur, C., Tarbouriech, S., Teel, A., and Zaccarian, L. (2019). A nonsmooth hybrid invariance principle applied to robust event-triggered design. *IEEE Transactions on Automatic Control*, 64(5), 2061–2068.

Strogatz, S.H. (2000). From Kuramoto to Crawford: Exploring the onset of synchronization in populations of coupled oscillators. *Physica D*, 143(1), 1–20.

Tass, P.A. (2003). A model of desynchronizing deep brain stimulation with a demand-controlled coordinated reset of neural subpopulations. *Biol. Cybern.*, 89(2), 81–88.

Wiesenfeld, K., Colet, P., and Strogatz, S.H. (1998). Frequency locking in Josephson arrays: Connection with the Kuramoto model. *Physical Review E*, 57(2), 1563–1569.